

Table S1. Sequences of the oligos and primers used

Oligo	Sequence
<u>Morpholinos</u>	
Random Sequence MO	CCT CTT ACC TCA GTT ACA ATT TAT A
<i>metAP2</i> MO	CAT GTC TTT ACC CAT CTT GCA CAG G
<i>metAP2-like</i> MO	CCT CAC CAT CTG TAA TGA AGT TTA C
<u>Primers for RT-PCR for MetAP2 mRNA in splice-site morpholino study</u>	
MetAP2 rtF	ACG CTG ATT TTA CCG AAT GG
MetAP2 rtR	TGC GTT GGG AGT GTA GTG AG
<u>Primers for the cloning of MetAPs in mRNA and riboprobe synthesis</u>	
MetAP1 F	TCT GAC CGA CAG CAG CAG AAG
MetAP1 R	TGA CTG GCT GAT CGG TGA TAT GG
MetAP2 F	ACA TAA TGG CAG ACG TGC AG
MetAP2 R	CCA CCT ACT GGC GTA ACG AT
MetAP2-like F	ACG CTG ATT TTA CCG AAT GG
MetAP2-like R	TGC GTT GGG AGT GTA GTG AG
<u>Primers for semi-quantitative RT-PCR</u>	
ZF β-actin F	TTC CTT CCT GGG TAT GGA ATC
ZF β-actin R	GCA CTG TGT TGG CAT ACA GG
MetAP1 F	AGG AGG GGG ACA TAT TGA AC
MetAP1 R	GTC TGA ACCAAT CTC TTG GC
MetAP2 F	TGG CCA CTC TAT TGG ACA GT
MetAP2 R	CTC GAT GGC ATA AAC CTC TC
MetAP2-like F	CCA TCT GTG ATC TGT ACC CC
MetAP2-like R	TCT CCT CAT CGC TCA TTC TC
<u>Primers For Q-RT-PCR</u>	
ZF β-actin F	TTC CTT CCT GGG TAT GGA ATC
ZF β-actin R	GCA CTG TGT TGG CAT ACA GG
ZF scl F	CTA TTA ACC GTG GTT TTG CTG G
ZF scl R	CCA TCG TTG ATT TCA ACC TCA T
ZF lmo2 F	GGA CGC AGG CTT TAC TAC AAA C
ZF lmo2 R	CCG GAT CCT CTT TTC ACA GGA A
ZF gata1 F	AAG ATG GGA CAG GCC ACT AC
ZF gata1 R	TGC TGA CAA TCA GCC TCT TTT

Oligo	Sequence
ZF eh α1 F	TGC TCT CTC CAG GAT GTT GA
ZF eh α1 R	TCA CAG TCT TGC CGT GTT TC
ZF eh β1 F	AGG CTC TGG CAA GGT GTC TCA
ZF eh β1 R	CAT TGG GTT TCC CAG GAT
ZF pu.1 F	GGG CAG TTT TAA CCA AAG ATC A
ZF pu.1 R	CCC AAG AGT GAT CGT TCT GAC
ZF l-plastin F	GAA GCT CTG ATC GCT CTG CT
ZF l-plastin R	GCT TCT TTT CAT CCG TCA GG
ZF mpo F	GGG GCA GAA GAA GAA AGT CC
ZF mpo R	CCC TTG CTA AAC TCT CAT CTC G
ZF c-myb F	TTT CTA CCG AAT CGA ACA GAT G
ZF c-myb R	CAA TCA CCC GTT GGT CTT CT
HU MetAP2 F	GTC TGT GTG ATG TTG GTG A
HU MetAP2 R	AAT CGG CAC TGT TTT TCC

Table S2. Fold-change of expression of *mpo* (18 hpf) and *c-myb* (48 hpf) in metap2-like^{MO}

Gene	Control	metap2-like^{MO}	p-value
<i>mpo</i>	1.00	1.23 ± 0.17	0.19
<i>c-myb</i>	1.00	1.09 ± 0.12	0.56

The data as shown represented average results of 3 experiments.

Figure S1. Amino acid alignment of MetAPs in different species

Sequences shaded in black or grey designate identical and similar residues respectively. Residues involved in the coordination of metal ions and in contact with fumagillin are labeled by closed and open arrowheads respectively. Underlined regions represent the insert region unique to the MetAP2 family. Putative zinc finger residues in human MetAP1 are marked by asterisks. Hs: *Homo sapiens*; Mm: *Mus musculus*; Dr: *Danio rerio*.

Figure S2. Bootstrapped phylogenetic tree generated with the neighbor-joining algorithm with 500 replicates

Values at each inner node represent bootstrap values, which is the percentage of replicates able to reconstruct the selected node. Hs: *Homo sapiens*; Mm: *Mus musculus*; Xl: *Xenopus laevis*; Dm: *Drosophila melanogaster*; Tn: *Tetraodon nigroviridis*.

Figure S3. Semi-quantitative PCR showing the expression of *metap2* at different developmental stages normalized with the expression level of β -actin

Figure S4

(A) DNA sequencing confirmed the molecular targeting of *metap2* MO. Bracket: Exon4 of *metap2* which is not present in defectively spliced *metap2* mRNA in metap2MO; Red circle: amino acid 106 where frame shift occur in metap2^{MO}; Green circle: amino acid 154 where premature stop occur in metap2^{MO}. (B) Defective splicing of *metap2* mRNA in metap2^{MO} as shown by RT-PCR at 48, 72, and 96 hpf. Wild-type *metap2* mRNA demonstrated by the 660 b.p. (black arrowhead) band gradually increased and became dominate again at 96 hpf while defectively-spliced *metap2* mRNA demonstrated by the 557 b.p. (red arrowhead) band gradually decreased. (C) Typical deformed embryos (less than 20% of total injected metap2^{MO}) after injection of *metap2* MO which were excluded from further analysis. Bars represent 250 μ m

Figure S5. Whole-mount ISH comparing expression of *scl*, *gata1*, α -*eHb* (lateral view), *pu.1* (lateral and ventral view), and *l-plastin* (ventral view) at 18 hpf between control and metap2^{MO}

Bars represent 250 μ m

Figure S6

(A) Whole-mount TUNEL assay comparing apoptosis between control and metap2^{MO} at 36 and 48 hpf in the trunk area. Bars represent 250 μ m

Figure S7

(A) Semi-quantitative PCR showing the expression of *metap1* and *metap2-like* at different developmental stages normalized with the expression level of β -actin. (B) Whole-mount ISH showing the spatial expression of *metap1* and *metap2-like* at different developmental stages. Bars represent 250 μ m

Figure S8

(A) Diagrammatic presentation of the action of the *metap2-like* morpholino. Red line represents the binding site of the splice-junction targeted *metap2-like* morpholino (B) DNA sequencing confirmed the molecular targeting of *metap2-like* MO. Purple bracket: Exon-2 of *metap2-like* ; Red bracket: Exon-3 of *metap2-like* which is not present in defectively spliced *metap2-like* mRNA in metap2MO; Green bracket: Exon-4 of *metap2-like*.

Figure S9

(A) Western blot showing the expression level of β -catenin in control, fumagillin treated embryos and metap2^{MO} at 18 hpf normalized to the expression level of β -actin. (B) Flow cytometry showing the percentage of gfp positive cell unaffected in Tg(*top:gfp*) embryos which is either injected with random sequence MO (control), treated with fumagillin or injected with *metap2* MO. Wt denotes Wild-type.

Figure S10

(A) Fluorescent microscopy of Tg(*fil1:gfp*) at 48 hpf comparing the development of development of dorsal aorta (DA), dorsal vein (DV) and intersegmental vessel (ISV) in the trunk region between control, MEK inhibitor treated embryos and metap2^{MO} co-treated with MEK inhibitor. (control: $97.1 \pm 1.2\%$ with normal ISV patterning in total 102 embryos; MEK inhibitor treatment: $83.8 \pm 2.7\%$ with perturbed ISV patterning in total 105 embryos; metap2^{MO} with MEK inhibitor treatment: $88.3 \pm 1.5\%$ with perturbed ISV patterning in total 77 embryos; n=3) (B) Whole-mount ISH comparing expression of *c-myb* at 36 hpf between control, MEK inhibitor treated embryos and metap2^{MO} co-treated with MEK inhibitor (control: $93.3 \pm 1.4\%$ with normal *c-myb* expression in total 90 embryos; MEK inhibitor treatment: $90.6 \pm 2.1\%$ with normal *c-myb* expression in total 85 embryos; metap2^{MO} with MEK inhibitor treatment: $80.2 \pm 4.4\%$ with reduced *c-myb* expression in total 86 embryos; n=3). Bars represent 100 μ m

Figure S11. Total number of colonies formed in colony-forming assay between control and fumagillin treated CB CD34⁺ cells

After 3 days treatment, 3000 cells (from vehicle) and cell numbers proportional to its expansion (fumagillin treated) were cultured in methylcellulose medium H4434 under the exposure of fumagillin for 14 days and total colonies numbers were counted.

Figure S12. Lineage analysis of human cells in engrafted mice

For CD34 and CD33, cells were co-stained with anti-CD45 and anti-CD34 or anti-CD33 antibodies respectively. Lineages were determined by CD45 positive and CD34 or CD33 positive fraction. For CD19, cells were single stained with anti-CD19 antibody. Lineage was determined by percentage of CD19-positive cells divided by CD45-positive cells (Figure 7F). N=3. N.A. indicates “not available” due to human engraftment is too low; N.D. indicates not done because mouse die before reaching harvesting time point.

Figure S1

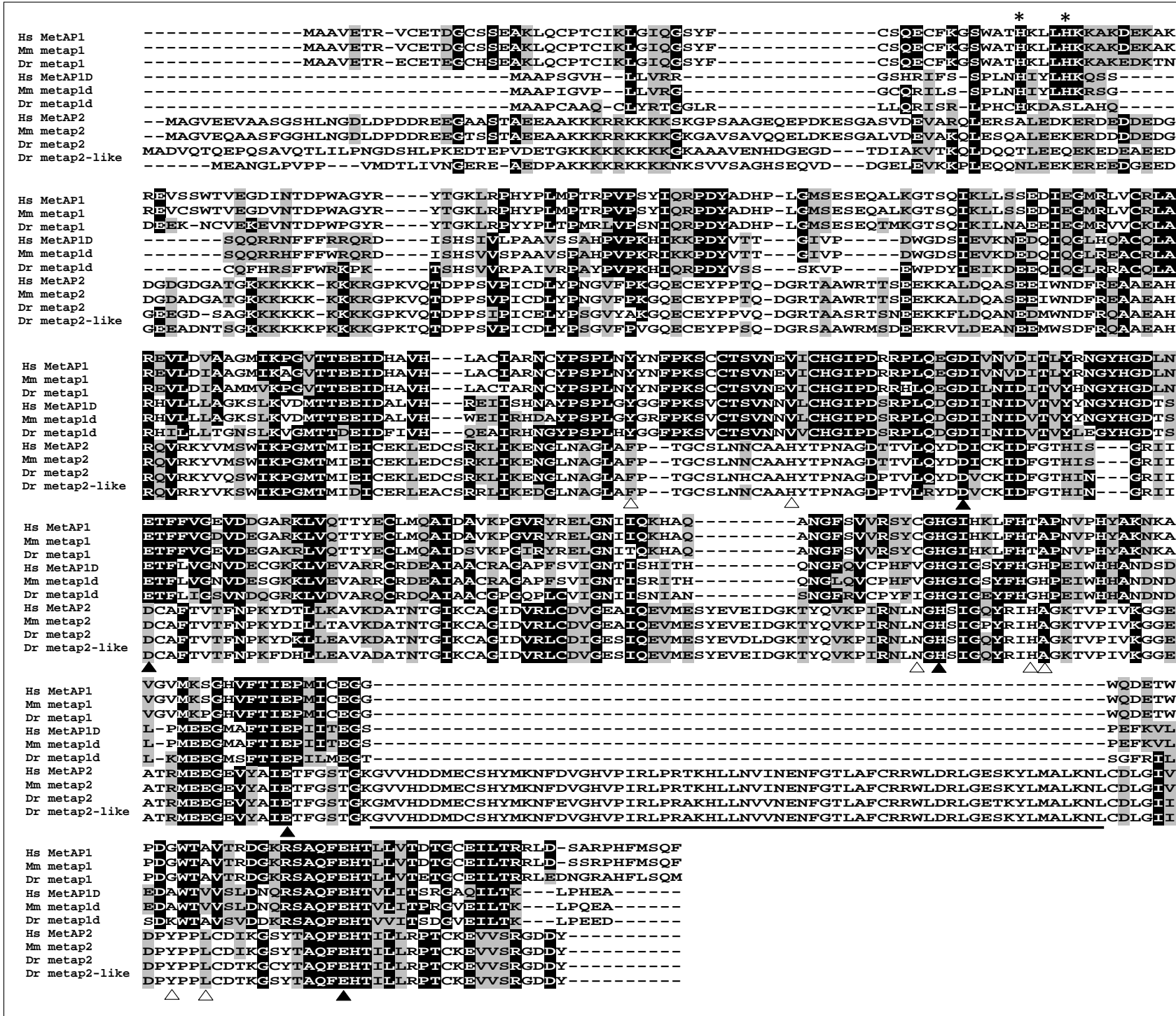


Figure S2

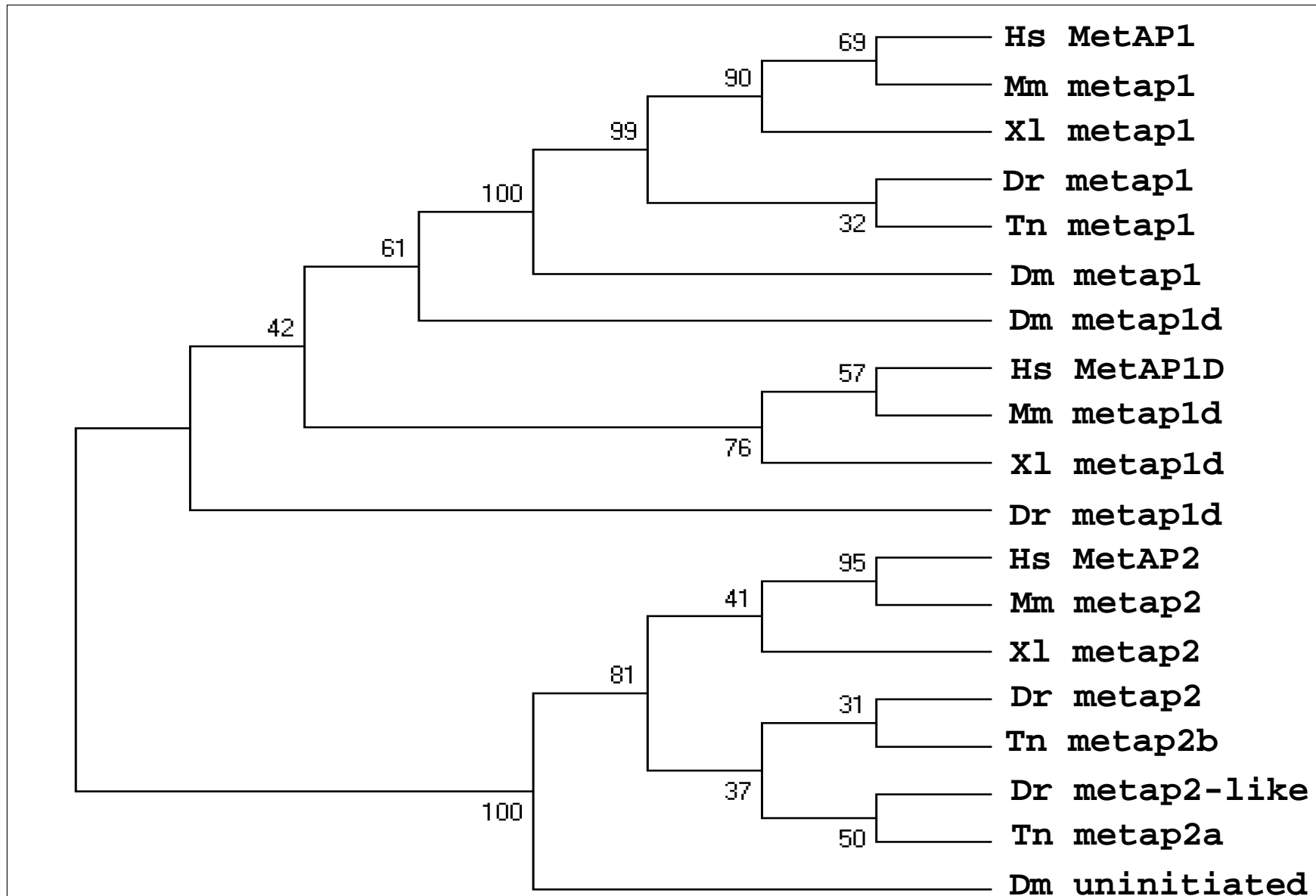


Figure S3

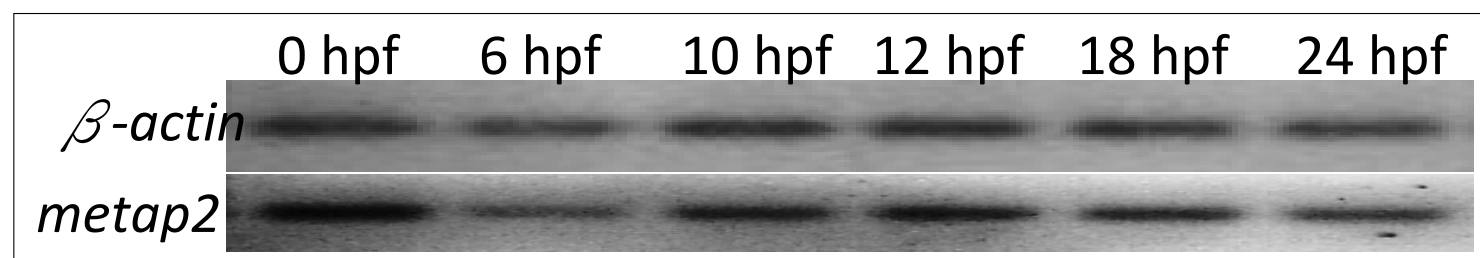
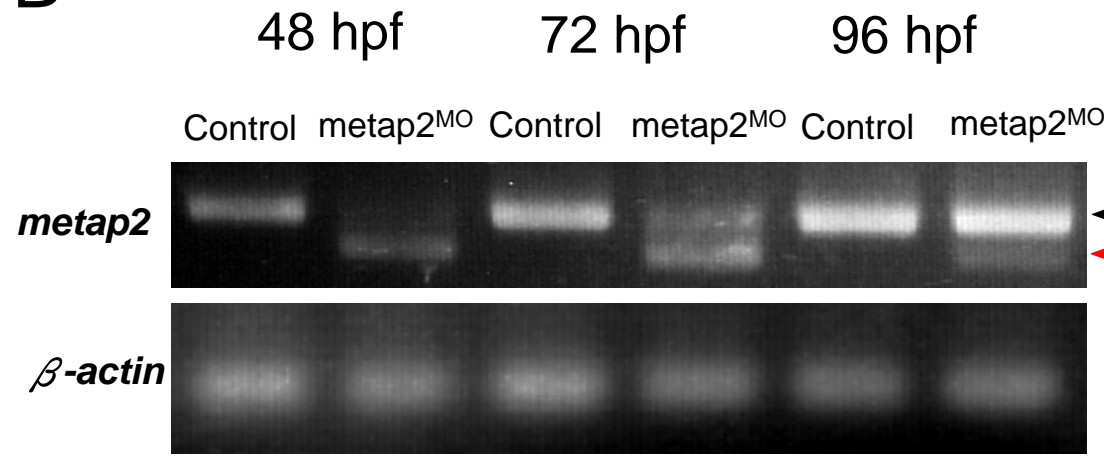


Figure S4

A

Wild-type	101	A A G A A G A A A A A G A A A G G C C	CC A A A G T G C A G A C A G A T C C G C C A T C T A T T C C C A T C T G T G A G
	K K K K K G P K V Q T D P P S I P I C E		
metap2^{MO}	101	A A G A A G A A A A A G A A A G G C C	- - - - -
	K K K K K G	(G)	
Wild-type	121	C T C T A C C C C A G T G G G A G T T T A T G C C A A G G G T C A G G A A T G T G A A T A T C C T C C T G T G C A A G A T	
	L Y P S G V Y A K G Q E C E Y P P V Q D		
metap2^{MO}	- - - - -		
Wild-type	141	G G A C G C A C G G G T G C T T C G C G A A C C A G C A A C G A A G A G A A G A A G T T T T G G A T C A G G G C G A A T	
	G R T A A S R T S N E E K K F L D Q A N		
metap2^{MO}	107	- - A C G C A C G G G T G C T T C G C G A A C C A G C A A C G A A G A G A A G A A G T T T T G G A T C A G G G C G A A T	
	H A R L L R E P A T K R R S F W I R R M		
Wild-type	161	G A G G A C A T G T G G A A T G A T T T C C G G C A G G G C C G A G G G C T C A C C G G C A G G T C A G G A A G T A C	
	E D M W N D F R Q A A E A H R Q V R K Y		
metap2^{MO}	127	G A G G A C A T G T G G A A T G A T T T C C G G C A G G G C C G A G G G C T C A C C G G C A G G T C A G G A A G T A C	
	R T C G M I S G R P P R L T G R S G S T		
Wild-type	181	G T G C A G A G G C T G G A T C A A A C C G G G A A T G A C C A T G A T C G A G A T T T G T G A G A A G C T G G A G G A C	
	V Q S W I K P G M T M I E I C E K L E D		
metap2^{MO}	147	G T G C A G A G G C T G G A T C A A A C C G G G A A T G A C C A T G A T C G A G A T T T G T G A G A A G C T G G A G G A C	
	C R A G S N R E * P * S R F V R S W R T	*	*

B



C Deformed *metap2^{MO}* 48 hpf

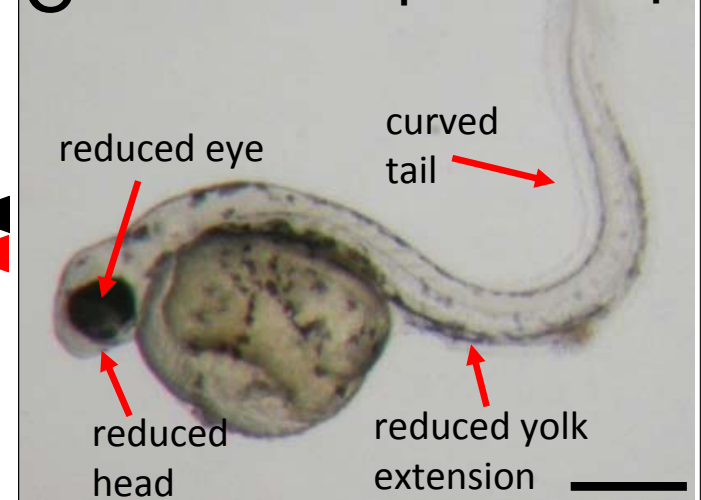


Figure S5

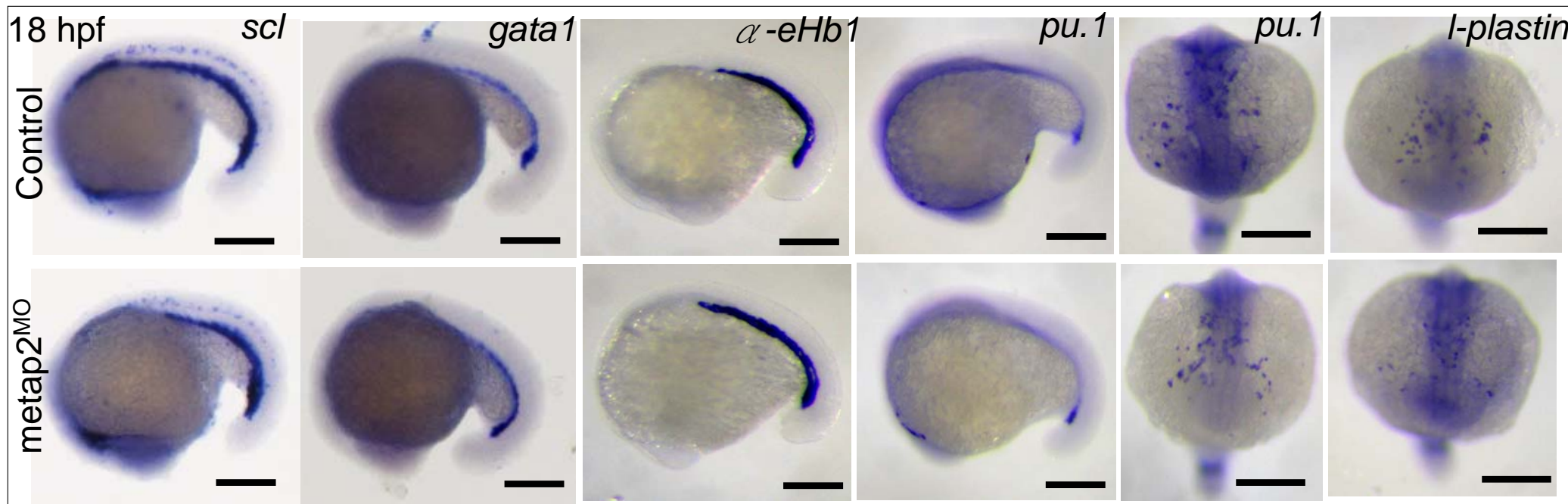


Figure S6

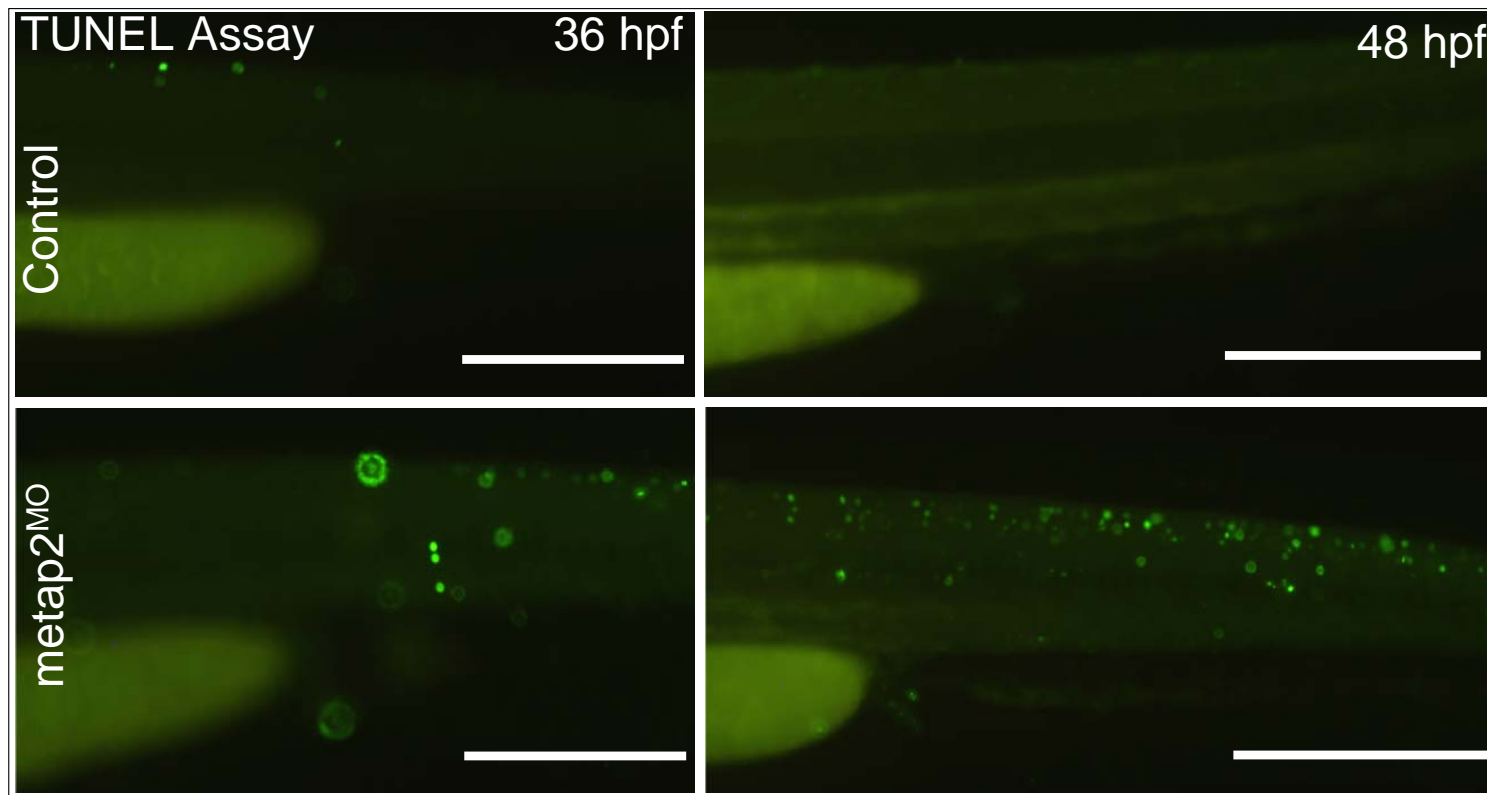


Figure S7

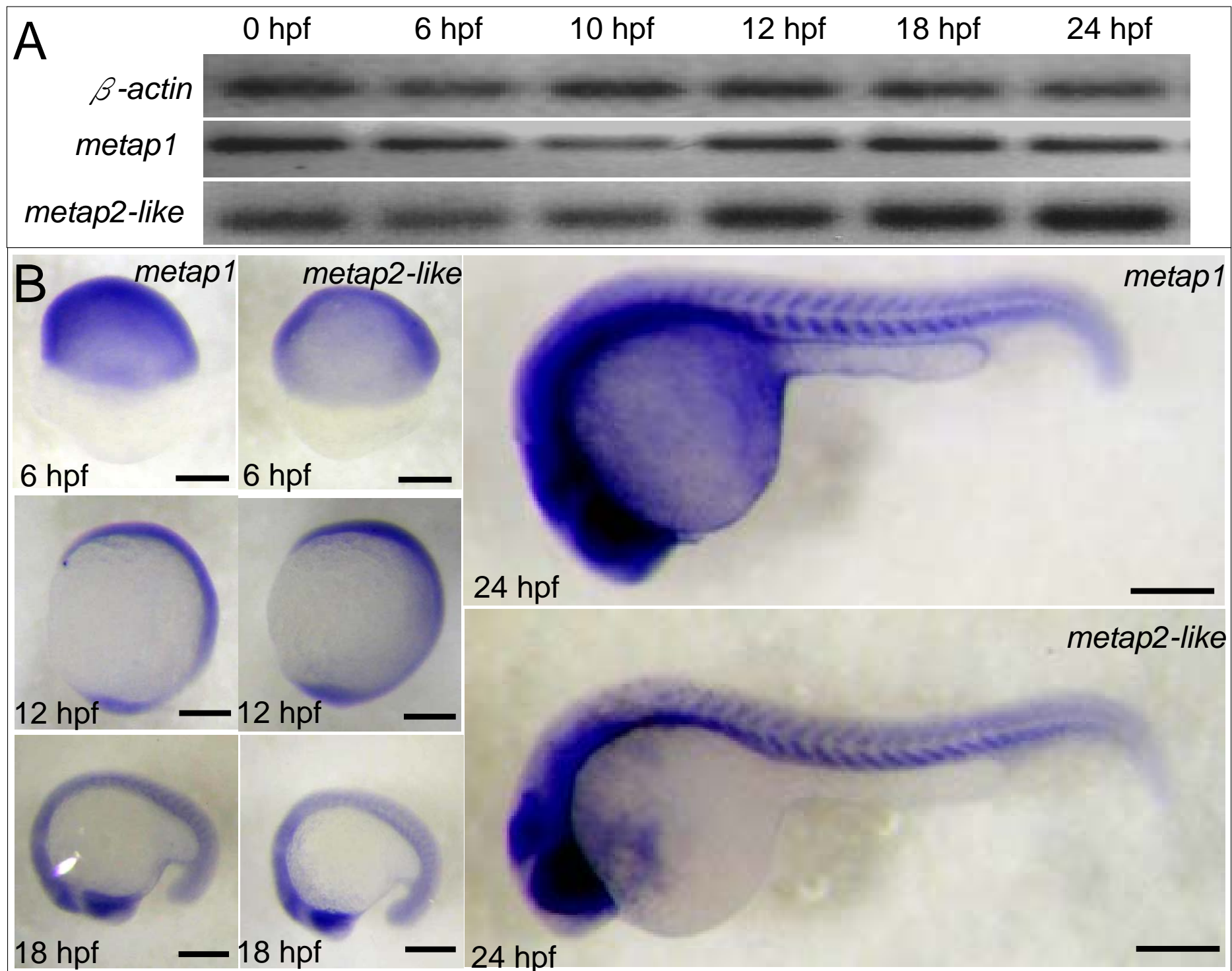
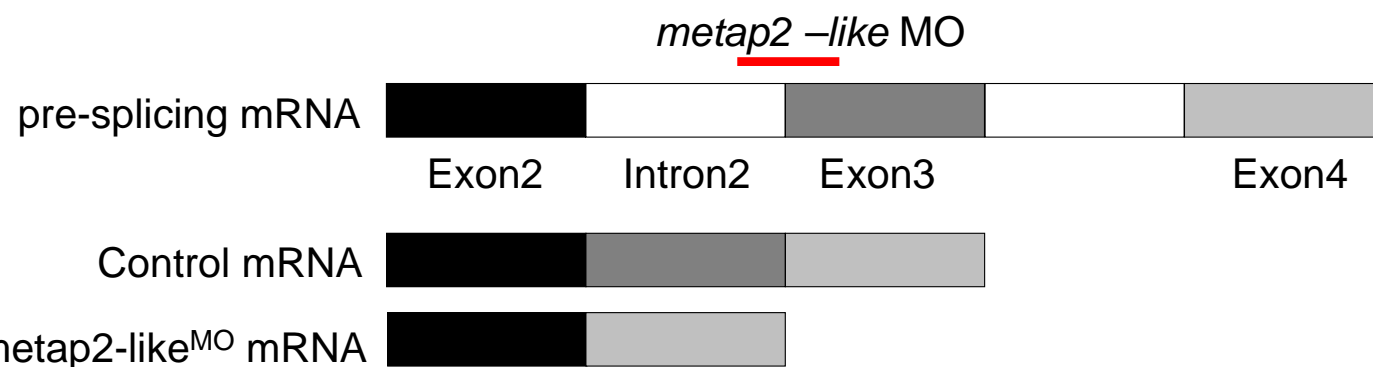


Figure S8

A



B Control

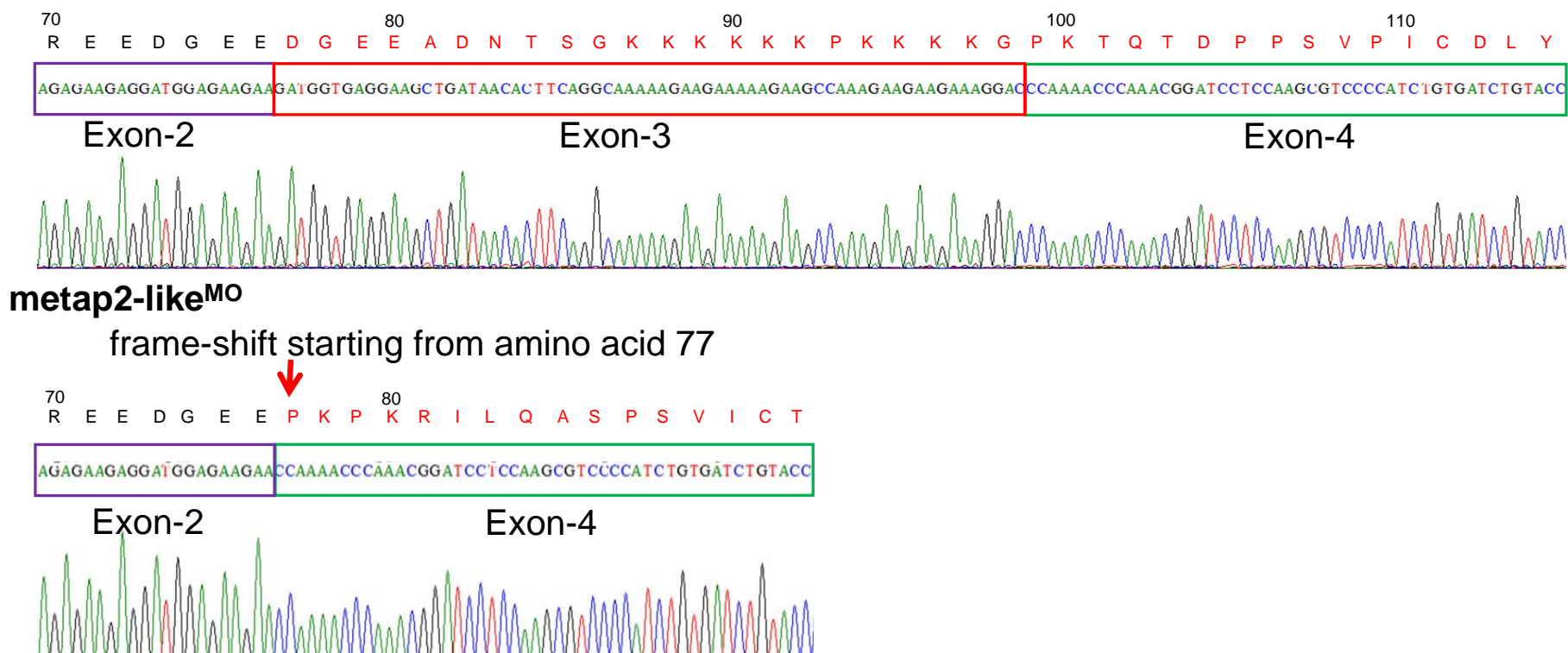


Figure S9

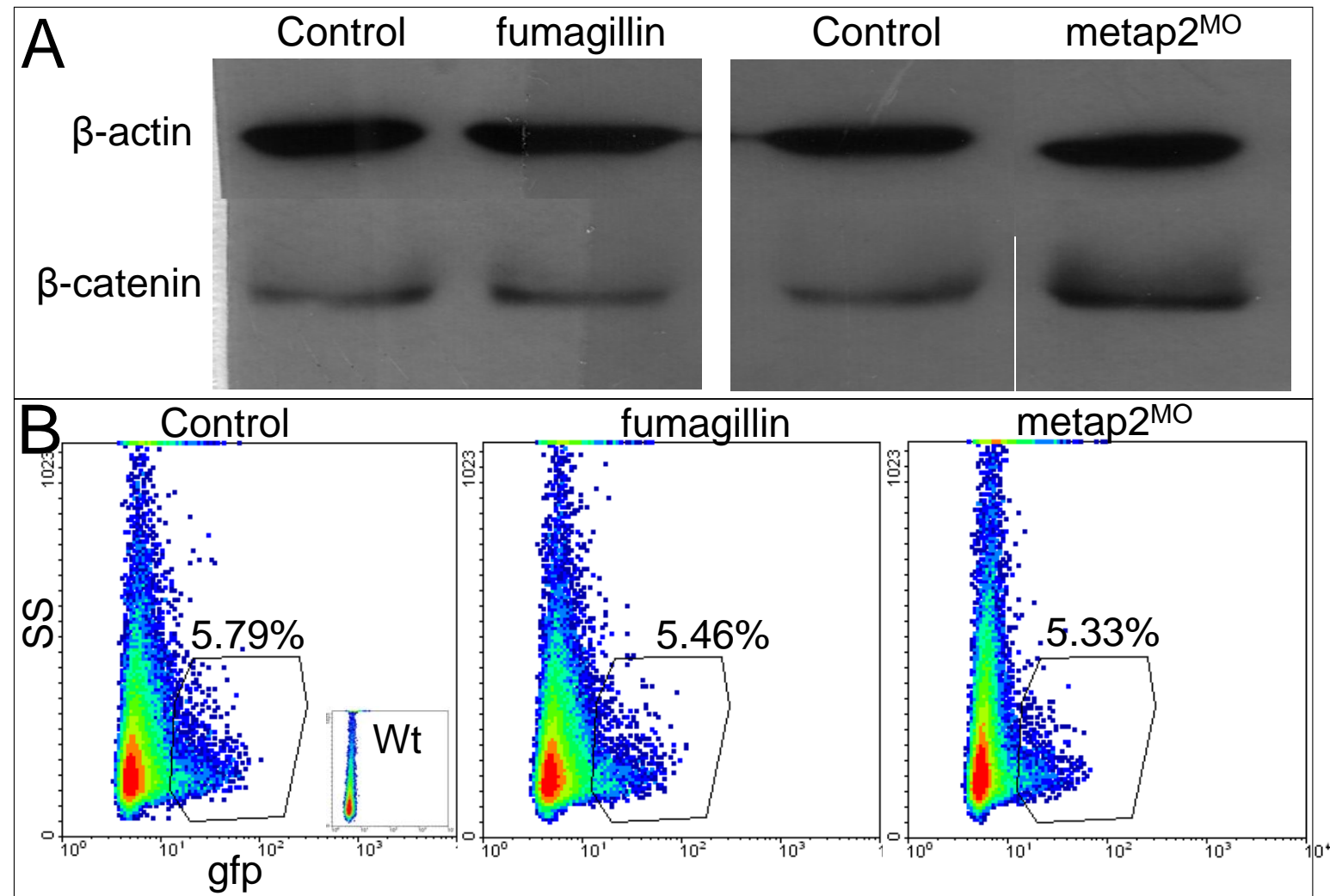


Figure S10

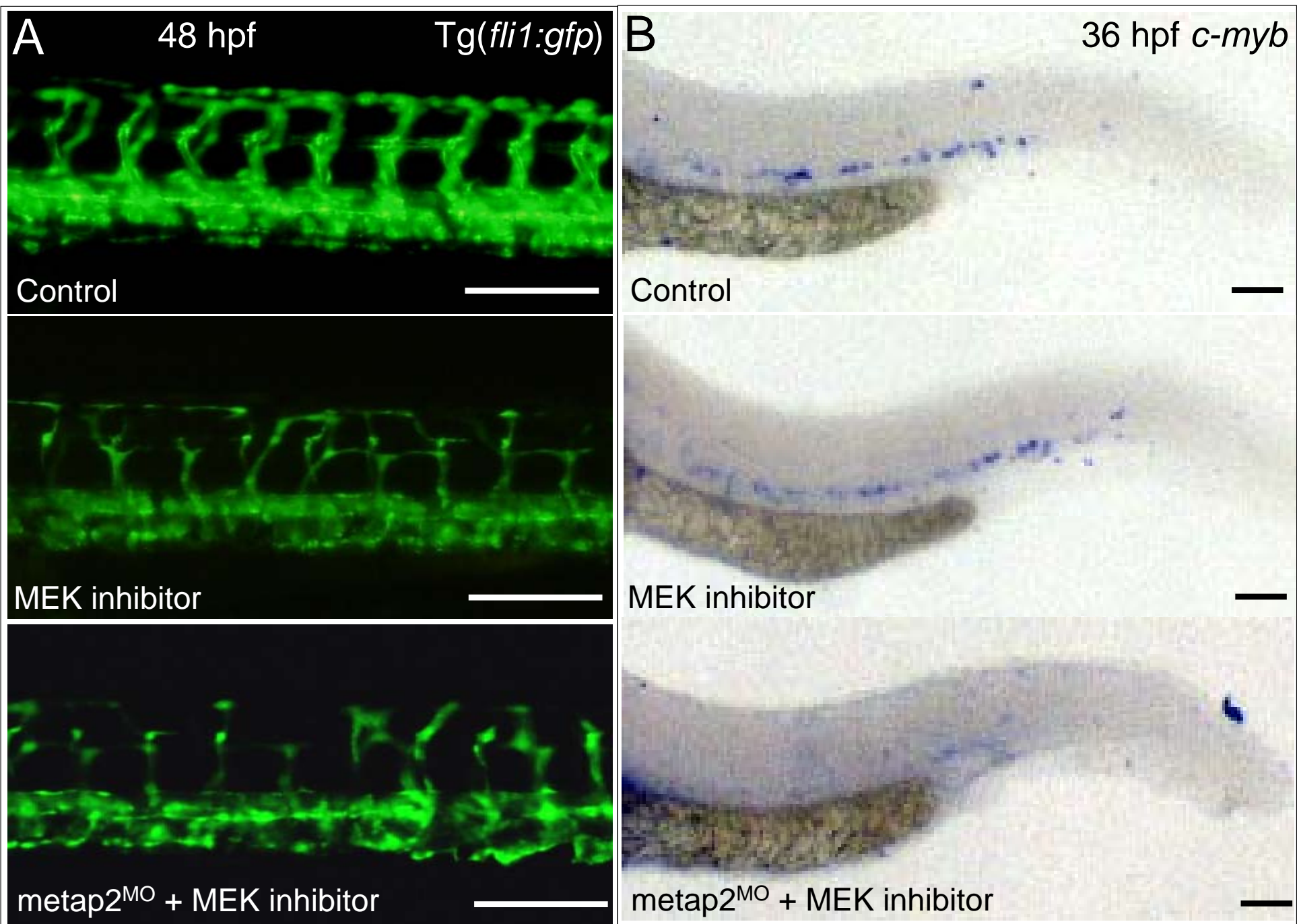


Figure S11

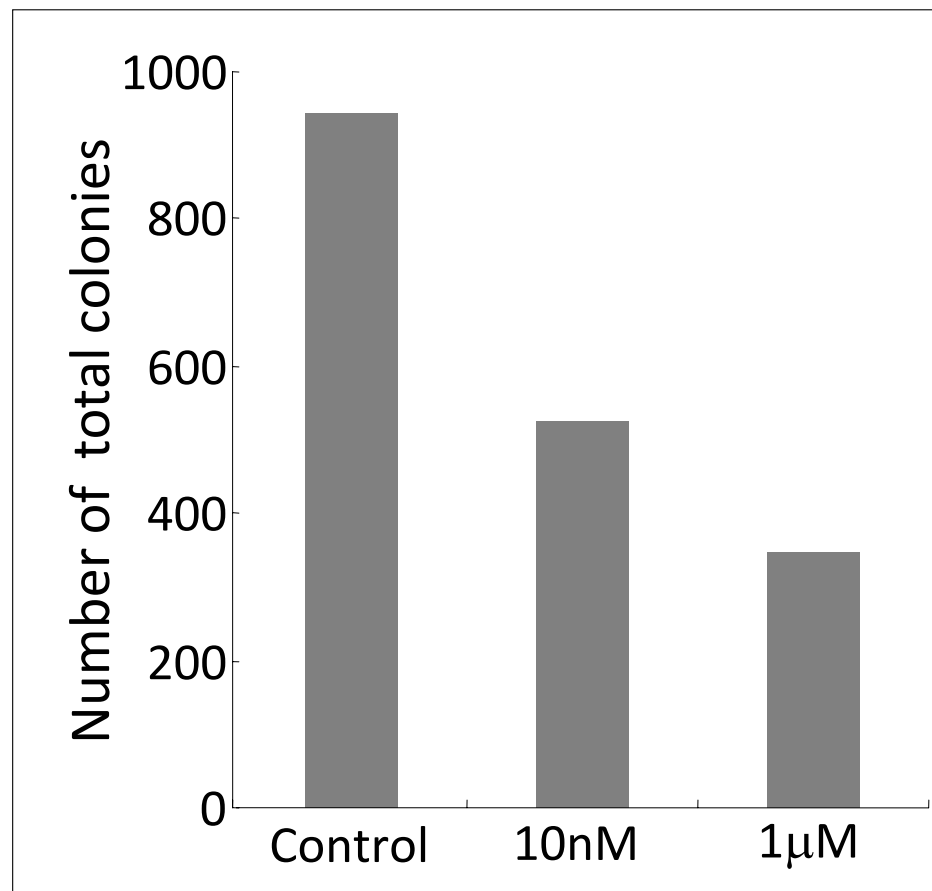


Figure S12

